

Composite ferromagnetic fabrics (magnetite, greigite) measured by AMS and partial AARM in weakly strained sandstones from western Makran, Iran

C. Aubourg and P. Robion

Laboratoire de Tectonique, UMR 7072, University of Cergy Pontoise, 8, Le Campus, 95031 Cergy, France. E-mail: charly.aubourg@geol.u-cergy.fr

Accepted 2002 June 5. Received 2002 June 5; in original form 2001 December 12

SUMMARY

We present examples of composite magnetic fabrics (AMS and partial AARM) in five sites from the western Makran accretionary prism. These rocks are weakly strained sandstones of Mio-Pliocene age. Rock magnetic investigations show a large occurrence of magnetite and also some greigite at two sites. Partial anhysteretic remanent magnetization coercivity spectra reveal that grain size is not homogeneous suggesting several grain fractions. AMS foliations are close to bedding, except at one greigite-bearing site where AMS foliation is almost perpendicular to bedding. Soft AARM (0–50 mT) foliations are slightly oblique both to bedding and AMS foliation. Surprisingly, hard AARM (50–100 mT) foliations are perpendicular to bedding. Comparison of two limbs of one fold suggests that AMS foliations are pre-tilting while hard-AARM foliations are post-tilting. Corrected degree of anisotropy parameters display similar trends for all sites ($P'_{\text{AMS}} \approx 1.04 < P'_{\text{softAARM}} \approx 1.11 < P'_{\text{hardAARM}} \approx 1.19$). We suggest that AMS, soft AARM and hard AARM reflect distinct magnetic grain populations. However, a possible relationship between hard AARM and a component of natural remanent magnetization is possible. Our study shows that two orthogonal fabrics exist in these weakly strained rocks; coarse grains are parallel to bedding, while fine grains are aligned perpendicular to bedding.

Key words: AMS, flysch, greigite, Makran, partial AARM.

INTRODUCTION

In fold and thrust belts, sedimentary rocks are generally weakly strained and only a few petrofabric elements such as bedding, fracture cleavage, tension gashes and brittle deformation can be recognized. It has been shown during the last four decades that magnetic fabric is a powerful approach to reveal some cryptic elements of the petrofabric (Graham 1954). Magnetic fabric appears as a precursor of visible strain (Borradaile & Henry 1997). Whilst AMS (Anisotropy of Magnetic Susceptibility) is the most popular method for measuring magnetic fabric, it has one principal drawback: AMS measures the combined contributions of diamagnetic, paramagnetic and ferromagnetic *sensu lato* susceptibilities (Hrouda 1982). The contribution of the ferromagnetic fraction alone can be characterized when using the anisotropic properties of remanent magnetization (Stephenson *et al.* 1986). Comparison between AMS and other remanence-related magnetic fabrics shows generally good agreement (Jackson 1991; Rochette *et al.* 1992; Aubourg *et al.* 2000). Only a few studies refer to qualitative and quantitative differences between AMS and remanence magnetic fabrics (Aubourg *et al.* 1995; Werner & Borradaile 1996; Robion *et al.* 1999; Rochette *et al.* 1999; Trindade *et al.* 1999).

McCabe *et al.* (1985) proposed to use the partial anisotropy of anhysteretic remanent magnetization (AARM). Anhysteretic remanent magnetization (ARM) is obtained by a combination of DC magnetic field (typically about 50 μT) and AC magnetic field (typically in the range 0–100 mT). There are two principal advantages of using ARM: 1) a low DC magnetic field (*ca.* 50–100 μT) is used. The acquisition curve of ARM vs DC field is expected to be linear in this range. This behavior is a desirable condition to measure a second order tensor of anisotropy (Daly & Zinsser 1973), 2) a window of AC field can be used to impart ARM. By measuring different windows of coercivity (partial AARM), one can expect to characterize different subpopulations (size and shape) of ferromagnetic grains. In this regard, Jackson *et al.* (1988) first documented multiple AARM magnetic fabrics by using different windows of coercive field. It was only a decade later that Trindade *et al.* (1999) explored again AMS and partial AARM in magnetite-bearing granites. To understand the advantage of using AMS in combination with partial AARM, let us consider schematically a grain size distribution and try to evaluate the grain size window measured by AMS, soft AARM, hard AARM and also the natural remanent magnetization (NRM). Put simply, it is important to remind ourselves that magnetic susceptibility of fine grains is less than that of coarse grains (if fine grains are not in the super-paramagnetic domain). Conversely,

the magnitude of remanent magnetization is greater for fine grains than for coarse grains. It thus appears that AMS and NRM tend to reflect different grain fractions, respectively coarse and fine. Soft and hard AARM grain fractions are in between AMS and NRM windows. The soft AARM grain population resembles the grain population that dominates AMS, while hard AARM is more representative of the grain population that carries NRM. There are two important comments that should be added to this simple view. First, grain fractions can overlap each other depending on the grain size distribution, and second the shapes of the grains (oblate vs prolate) and their composition (if there are two, or more, species of ferromagnetic grains) also play a role.

In this paper, we investigate AMS and partial AARM in order to test whether the petrofabric of magnetic grains is the same for all grain fractions. The rocks studied are weakly strained sandstones from the Makran accretionary prism. We show that coarse grains lie within (or closely parallel) the bedding while fine grains have a magnetic foliation perpendicular to bedding.

METHODS

All magnetic fabric measurements (AMS, pAARM) were carried out at the Department of Earth Sciences (University of Cergy Pontoise). Magnetic fabric is qualitatively defined by the orientation of principal susceptibilities or pAARM susceptibilities ($K_1 > K_2 > K_3$). K_1 , K_3 and the magnetic foliation (plane $K_1 - K_2$) are plotted in equal-area downward projections. We use the corrected degree of anisotropy P' and the shape parameter T (Tarling & Hrouda 1993) to quantify the magnitude and the shape of the ellipsoid. AMS was measured with a Kappabridge KLY2 (Agico) using fifteen positions according to Jelinek (1977). Anhysteretic magnetization was imparted with a DC field of 100 μT and AC field in the range 0 to 100 mT, using the AF demagnetizer LDA1 (Agico Ltd.). A tumbling system is used to demagnetize the sample after each position. Soft and hard AARM are measured respectively within the window 0–50 mT and 50–100 mT. Hard ARM (50–100 mT) is obtained by applying an ARM at 100 mT and demagnetizing the resulting ARM at 50 mT by using a computer-controlled 3-axis tumbler. ARM was measured with a spinner magnetometer JR5 (Agico Ltd.). To compute the AARM tensor, we used the Jelinek (1993) protocol. This protocol utilizes six independent positions. Each position is measured twice with opposite magnetization in order to correct the signal for the residual natural remanent magnetization. To test the reliability of AARM measurements, we carried out several tests.

(1) We monitored the viscosity of imparted ARM. We found that stability of ARM is reached after 1 min. Thus, we measured each imparted ARM after one to two minutes.

(2) We have performed acquisition curves of ARM in DC fields ranging from 5 μT to 500 μT (AC field of 100 mT) for one representative sample of each site (Fig. 1). In the mean time, we measured opposed ARMs imparted along the $+z$ and $-z$ axes (z : long axis of the 10.8 cc core) and corrected them for residual natural magnetization. We derived from these two measurements the error percentage of opposite ARM ($E = 200 \times (\text{ARM}_{\text{max}} - \text{ARM}_{\text{min}}) / (\text{ARM}_{\text{max}} + \text{ARM}_{\text{min}})$ per cent, where ARM_{max} and ARM_{min} are the maximum and minimum value of the opposed ARMs). ARM acquisition curves show good linearity up to 200 μT (Fig. 1). For DC fields lower than 20 μT , the consistency of opposed ARM is rather poor ($E > 4$ per cent). At 100 μT , the consistency of opposed ARM is very good at site Z71 and remains acceptable (1 per cent $< E < 3$ per cent) for other sites.

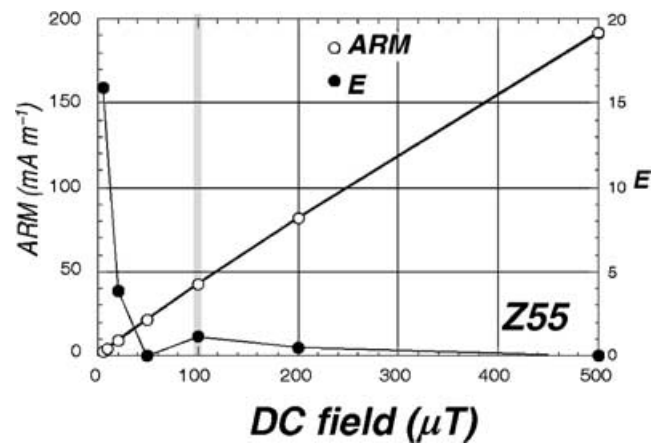


Figure 1. Acquisition of anhysteretic remanent magnetization (ARM) and test consistency parameter for opposed ARMs, E ($E = 200 \times (\text{ARM}_{\text{max}} - \text{ARM}_{\text{min}}) / (\text{ARM}_{\text{max}} + \text{ARM}_{\text{min}})$ per cent). We measured at each incremental DC field paired ARMs along $+Z$ and $-Z$ axes of the core. The thick grey line corresponds to the selected DC field for measuring AARM.

(3) We measured AARM of the same sample three times. We always found good agreement and reproducibility for the sites presented in this study.

(4) We checked the orientation of partial AARM axes in core coordinates in order to detect any bias as reported by Tauxe *et al.* (1990). We conclude that there is no relationship between core axes and partial AARM axes.

In addition to magnetic fabrics, we measured thermomagnetic curves ($K-T$ curves), stepwise demagnetization of composite isothermal remanent magnetization (IRM), hysteresis loops, and coercivity spectra of partial ARM of representative samples. $K-T$ curves were measured under argon with a kappabridge KLY-3 coupled with the CS-3 furnace. Stepwise demagnetization of composite IRM imparted successively along orthogonal axis at 1.2 T, 0.5 T, 0.1 T were performed according to the method proposed by Lowrie (1990). Hysteresis cycles are determined using a Micromag Vibrating Sample Magnetometer. We determined real partial ARM coercivity spectra on standard cores (10.8 cc) in steps of 5 mT according to the method of Jackson *et al.* (1988).

PRESENTATION OF SITES AND ROCK MAGNETISM

Sites Z55, Z60, Z64, Z71 and Z109 are located in the western part of the Makran, south East Iran (Fig. 2). It consists of Neogene weakly strained grey sandstones derived from the formation of the Makran accretionary prism, which is still active (McCall 1997). Sites Z55 and Z109 belong to thick Mio-Pliocene flysch series. Sites Z60, Z64 and Z71 are proximal continental rocks. Z55, Z60, Z64 and Z71 are located in a gentle flank of kilometric ramp-related folds (Fig. 2). Z109 is sampled in the two limbs of a 500-m length fold. Brittle deformation is very scarce, and only rare tension gashes are observed. No cross-bedding or internal deformation is visible in the field. Thin section of one representative sample from site Z55 (Fig. 3) shows a quartz matrix with carbonates, clays and a relative abundance of large opaque minerals. Opaque minerals are rounded, and are therefore likely of detrital origin. Magnetic susceptibilities range from $1 \cdot 10^{-4}$ SI to $2 \cdot 10^{-3}$ SI (Table 1). Soft anhysteretic susceptibility ($1 \cdot 10^{-4}$ SI to $2 \cdot 10^{-3}$ SI) is of the same order as

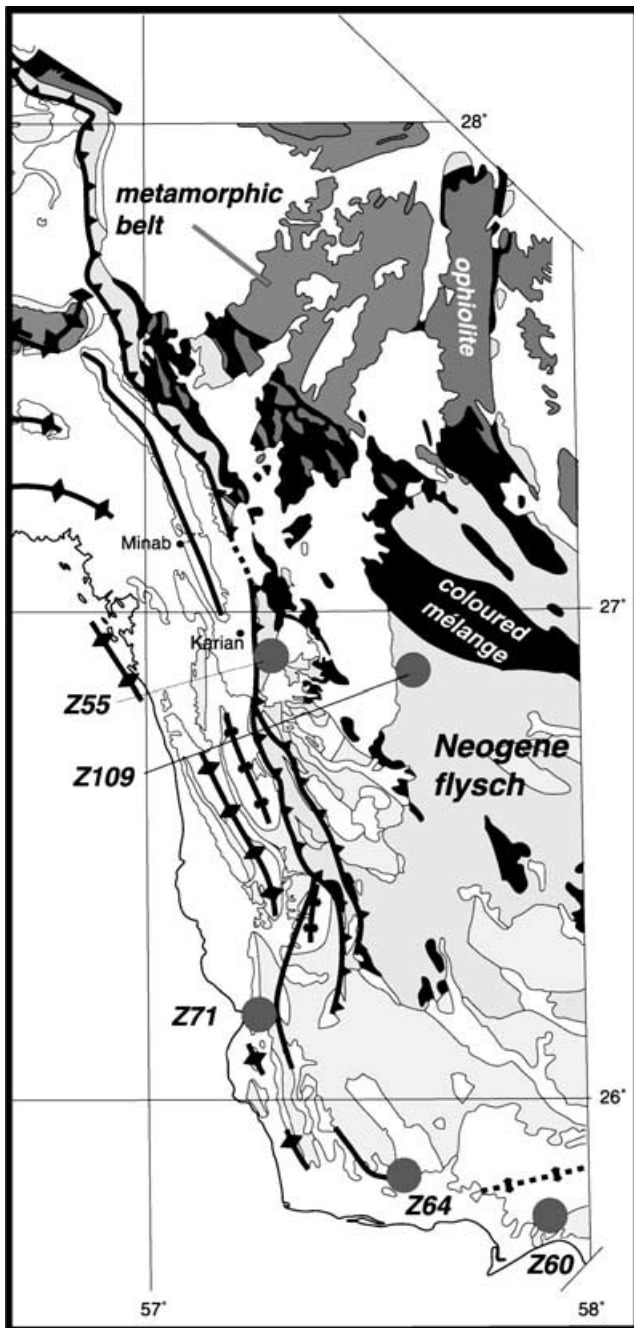


Figure 2. Map of the western part of Makran showing site location. Trends of fold axes and main faults are shown, defining the bending of the Makran prism.

magnetic susceptibility and higher than hard anhysteretic susceptibility ($5 \cdot 10^{-5}$ SI to $5 \cdot 10^{-4}$ SI) (Table 1). Hysteresis loops show that ferromagnetic susceptibility is significantly larger than high-field magnetic susceptibility, which represents at most 10 per cent of the initial susceptibility. Hysteresis ratios ($2.25 < H_{cr}/H_c < 3.63$ and $0.11 < J_{rs}/J_s < 0.23$, where M_{rs} is the saturation remanence, M_s is the saturation magnetization, H_{cr} is the coercivity of remanence, H_c is the coercive force) plot in the PSD field of to Day *et al.* (1977).

Stepwise thermal demagnetization of 3-axis composite IRMs exhibits very similar signatures for all sites (Fig. 4a). They are charac-

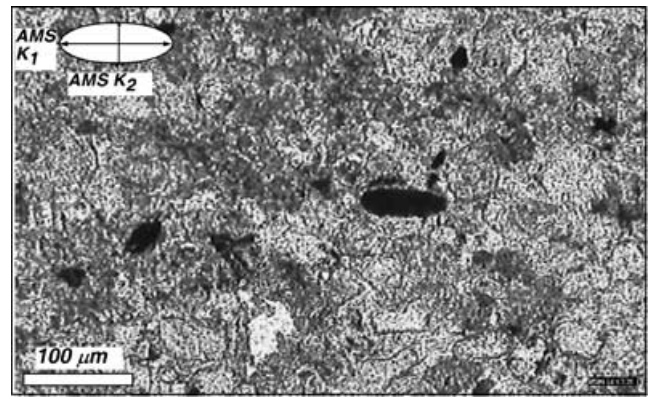


Figure 3. Thin section (natural light) at site Z55 parallel to the AMS foliation (K_1 – K_2 plane). A matrix of quartz and carbonates and opaque minerals (essentially magnetite and greigite) is observed. Note the rounded shape of opaque minerals that suggest a detrital origin.

terized by dominance of soft coercivity, with maximum unblocking temperatures below 600°C . Magnetite is therefore the main ferromagnetic fraction. This is confirmed by K – T curves (Fig. 4b), which show Curie temperature close to 580°C , indicating a Ti-poor magnetite. Note that no paramagnetic trend is observed at low temperatures on the K – T curve (Fig. 4b). This, together with relatively low high-field magnetic susceptibility, suggests that ferromagnetic susceptibility dominates the low-field magnetic susceptibility in the studied sandstones. The slope change for the soft IRM component at about 300°C (Fig. 4a) is also expressed in K – T curves at sites Z55 and Z60 (Fig. 4b). Because the same intermediate Curie temperature is detected at 360°C in both sites, we believe that this secondary mineral is not titanium-rich magnetite. This Curie temperature of 360°C is close to the Curie temperature of the iron sulfide greigite as reported by Sagnotti & Winkler (1999). Additional arguments suggest the presence of greigite rather than any other iron sulfide such as pyrrhotite. 1) We found that samples Z60 and Z55 samples are sensitive to gyroremanence (Stephenson 1993) when they are submitted to static AF demagnetization (results are not shown). 2) Samples are sensitive to the test of field impressed AMS anisotropy (Sagnotti & Winkler 1999) after saturating the core along the z-axis with a DC field of 1.2 T. Increase of magnetic susceptibility is about $100 \mu\text{SI}$ (~ 3 per cent) and $50 \mu\text{SI}$ (~ 6 per cent) respectively at sites Z55 and Z60. 3) Additional K – T curves under argon show that greigite is rapidly destroyed from 360°C to make magnetite at both sites.

In order to illustrate the magnetic grain distribution, we show the coercivity spectrum of partial ARM for greigite-bearing (site Z60) and magnetite-bearing (site Z64) samples (Fig. 5). To test this statistical reliability of the partial ARM spectra, we measured several samples and also the same sample three times. The distinguishable peak at about 15 mT suggests the occurrence of large grains according to Jackson *et al.* (1988). Interestingly, several additional peaks are suggested (Fig. 5), indicating that grain size range is not narrow and unimodal. The same pattern of partial ARM is observed at all sites.

In summary, rock magnetic investigation indicates that ferromagnetic grains dominate the low field magnetic susceptibility, and thus AMS. Ti-poor magnetite is the main mineral at sites Z71, Z64 and Z109 while greigite is also detected at sites Z55 and Z60. A broad grain size distribution is indicated by pARM coercivity spectra.

Table 1. Mean anisotropy data.

Sites	n AMS	n AMS heated	n Soft AARM	n Hard AARM	P'AMS	S	P'AMS heated	S	P'AAARM-s	S	P'AAARM-h	S	TAMS	S	TAMS heated	S	TAAARM-s	S
Z55	5	6	4	5	1.090	0.028	1.062	0.013	1.188	0.038	1.188	0.051	0.740	0.160	0.720	0.090	0.280	0.320
Z60	5	6	4	4	1.042	0.013	1.045	0.010	1.148	0.017	1.148	0.087	0.840	0.220	0.610	0.240	0.030	0.400
Z64	5	*	4	5	1.022	0.010	*	*	1.054	0.027	1.155	0.050	0.190	0.330	*	*	0.115	0.590
Z71	5	*	3	6	1.023	0.010	*	*	1.074	0.020	1.150	0.040	0.550	0.430	*	*	0.000	0.400
Z109-gentle	4	*	4	4	1.044	0.011	*	*	1.079	0.020	1.214	0.118	0.313	0.440	*	*	0.006	0.260
Z109-steep	4	*	4	4	1.038	0.010	*	*	1.135	0.032	1.234	0.101	0.097	0.350	*	*	0.122	0.380
TAAARM-h	S	KAMS	S	KAAARM-s	S	KAAARM-h	S											
0.030	0.310	2510	858	2100	127	474	59											
0.190	0.330	2620	249	2010	52	151	99											
0.000	0.230	642	272	138	463	302	43											
0.360	0.340	193	23	540	30	174	12											
0.096	0.160	185	36	117	5	46	9											
-0.220	0.260	180	14	137	1	52	7											

not heated.

n : number of samples.

P'AMS = corrected degree of anisotropy parameter for low field magnetic susceptibility;

P'AAARM-s = corrected degree of anisotropy parameter for soft fraction (0–50 mT) of anystheretic remanent magnetization;

P'AAARM-h = corrected degree of anisotropy parameter for hard fraction (50–100 mT) of anystheretic remanent magnetization;

TAMS = anisotropy shape parameter for low field magnetic susceptibility measurements;

TAAARM-s = anisotropy shape parameter for soft fraction of anystheretic remanent magnetization;

TAAARM-h = anisotropy shape parameter for hard fraction of anystheretic remanent magnetization;

KAMS = mean susceptibility (10⁻⁶ SI);

KAAARM-s = mean anystheretic susceptibility (10⁻⁶ SI) for soft coercivities (0–50 mT);

KAAARM-h = mean anystheretic susceptibility (10⁻⁶ SI) for hard coercivities (50–100 mT);

S standard deviation (10⁻⁶ SI);

T = 2(η₁ - η₂)/(η₂ - η₃) - 1; P' = exp(√2[(η₁ - η_m)² + (η₂ - η_m)² + (η₃ - η_m)²]), η_i = ln K_i, η_m = (η₁ + η₂ + η₃)/3.

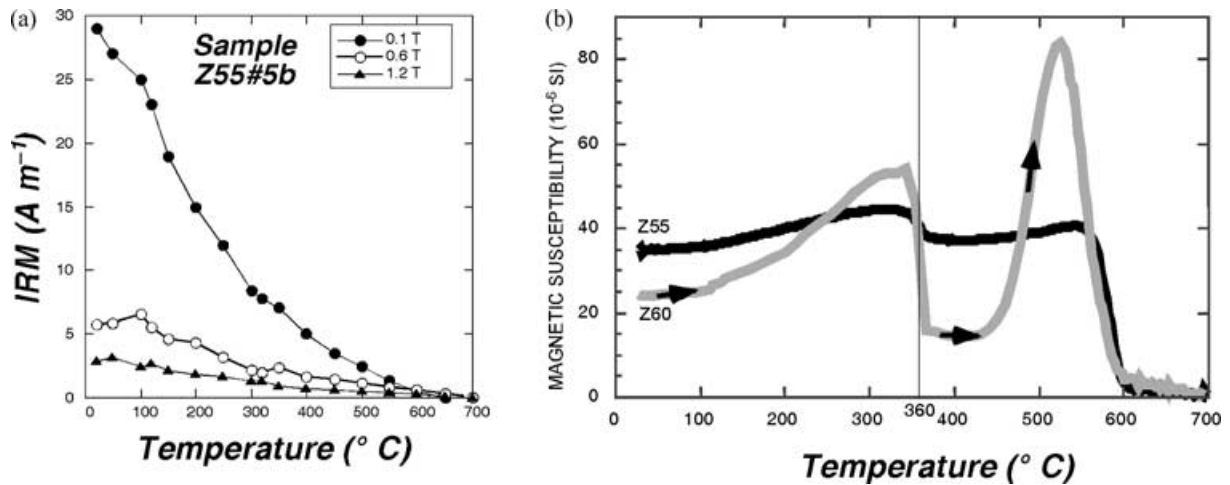


Figure 4. (a) Representative stepwise thermal demagnetization of isothermal remanent magnetization (under air) is shown. Note the dominance of soft coercivity (<0.1 T), the unblocking temperature at about 580°C, which is typical of magnetite, and the slope change at about 300°C. (b) $K-T$ curve under argon of sample from sites Z55 and Z60. One can see a Curie temperature at about 360°C, which is due to greigite (see text) and another Curie temperature at 580°C. Greigite is completely destroyed after heating.

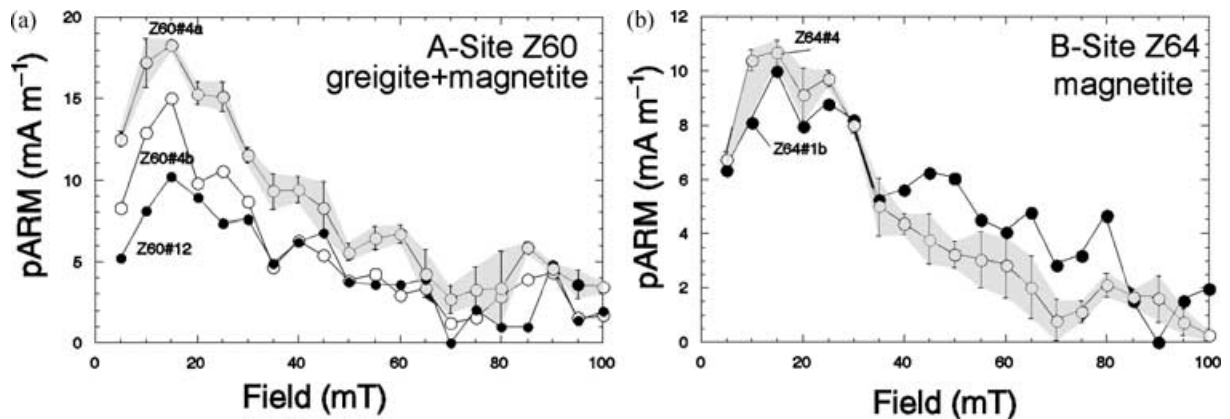


Figure 5. Partial anisotropic remanent magnetization coercivity spectra. Partial ARM coercivity spectrum are measured, according to the method of Jackson *et al.* (1988) in steps of 5 mT. Error bars correspond to standard deviations computed from three measurements of pARM. Note the occurrence of several peaks, which suggests several grain size population in the rocks.

Coarse detrital magnetites derived probably from alteration of ultrabasics and volcanics, located in the coloured mélangé (McCall 1997). Greigite is generally attributed to anoxic conditions during late diagenesis conditions (Sagnotti & Winkler 1999).

MAGNETIC FABRIC RESULTS

We measured AMS, soft and hard AARM of 3 to 6 samples. 90 per cent of the samples have individual confidence angles less than 10°. These confidence angles are routinely computed from Jelinek methods (Jelinek 1978). We present first magnetite-bearing samples (sites Z64, Z71, fold Z109), and then greigite-bearing sites (Z55, Z60).

At sites Z64 and Z71, AMS foliations are respectively parallel and slightly oblique to bedding (Fig. 5). In both sites, we observe the following characteristics: Soft AARM foliation is slightly oblique to bedding and AMS foliation; hard AARM foliation is perpendicular to bedding; anisotropy parameters of AMS display rather oblate shape and weak anisotropy while soft and hard AARM show stronger

anisotropy and rather triaxial shape. Note that soft AARM is less anisotropic than hard AARM.

At fold Z109 (Fig. 7), we have the opportunity to test magnetic fabric in respect to geometry of gentle and steep limbs. To visualize the grouping of magnetic fabric axis, we plot the tensorial mean according to Jelinek (1978). When comparing AMS in geographic coordinates and after bedding correction, we see that AMS foliation is pre-tilting and equally oblique to bedding in both limbs (Fig. 7a). AMS lineation is roughly parallel to the intersection of magnetic foliations. In gentle limb (Fig. 7b), soft and hard AARM are scattered. AMS, and soft and hard AARM are slightly clockwise rotated respectively from each other. Conversely, magnetic fabrics in steep limb (Fig. 7b) are better defined. AMS and partial AARM lineations are more or less parallel each other. However, magnetic foliations rotate progressively. We observe that soft AARM foliation lies between AMS and hard AARM foliations. Despite scattering, one can note that hard AARM foliations in both limbs of the folds are close each other. This contrasts with AMS foliations that are clearly pre-tilting. Anisotropy parameters P' and T have the same trend in both limbs (Fig. 7b), and reflect the same pathway to those observed at magnetite-bearing sites Z64 and Z71.

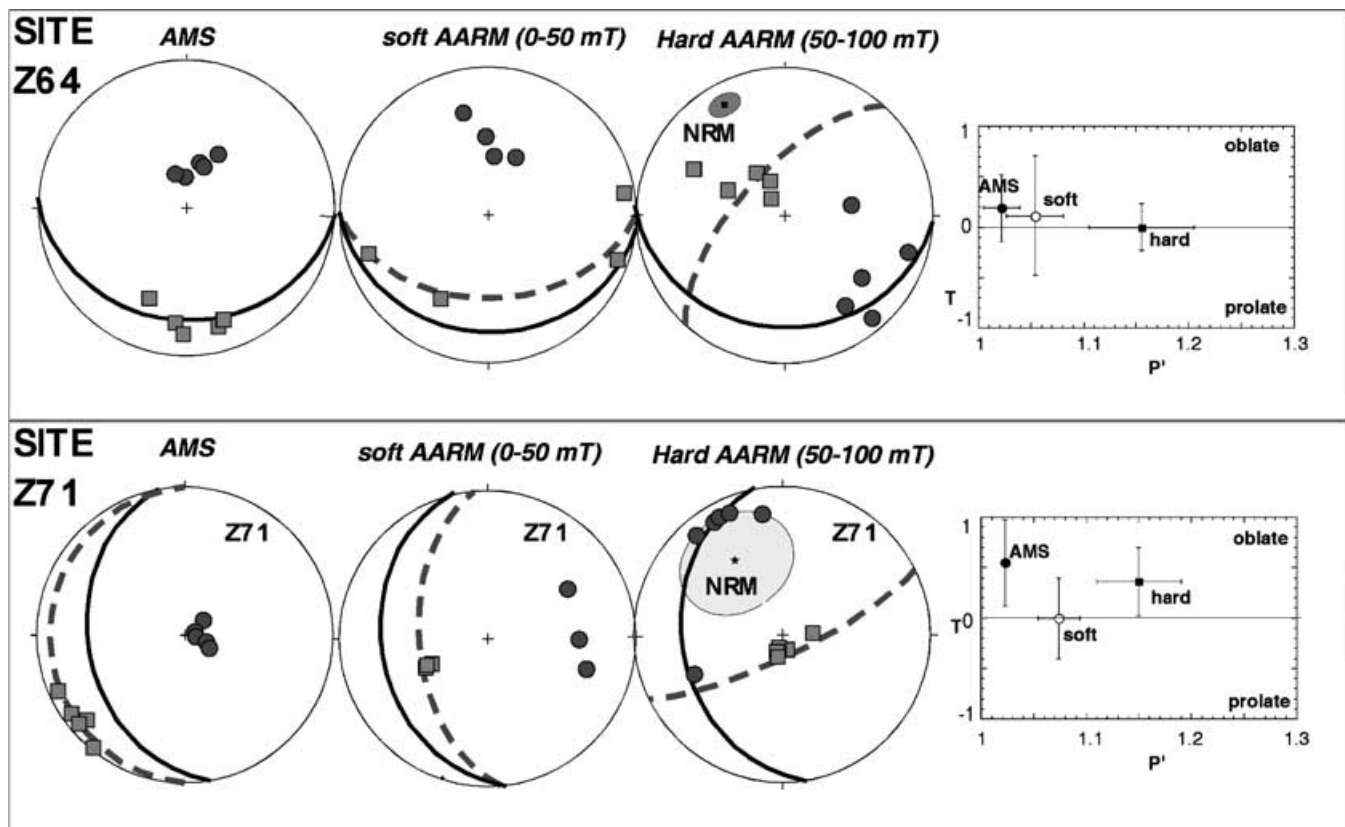


Figure 6. Magnetic fabrics (AMS, soft AARM (0–50 mT) and hard AARM (50–100 mT) for magnetite-bearing sites Z64 (a) and Z71 (b). Maximum (K_1 = full squares) and minimum (K_3 = circles) magnetic fabric axes are plotted in geographic coordinates in downward stereographic equal-area projection. Bedding (thick great circle) and magnetic foliation (dashed great circles) are shown. The intermediate temperature component of NRM is shown for hard AARM. Arithmetical mean of anisotropy parameters P' and T are displayed with their standard deviation. T : shape of the ellipsoid $T = 2(\eta_1 - \eta_2)/(\eta_2 - \eta_3) - 1$; -1 : prolate, $+1$ oblate, 0 : triaxial). P' : corrected degree of anisotropy $P' = \exp(\sqrt{2[(\eta_1 - \eta_m)^2 + (\eta_2 - \eta_m)^2 + (\eta_3 - \eta_m)^2]})$, $\eta_i = \ln K_i$, $\eta_m = (\eta_1 + \eta_2 + \eta_3)/3$.

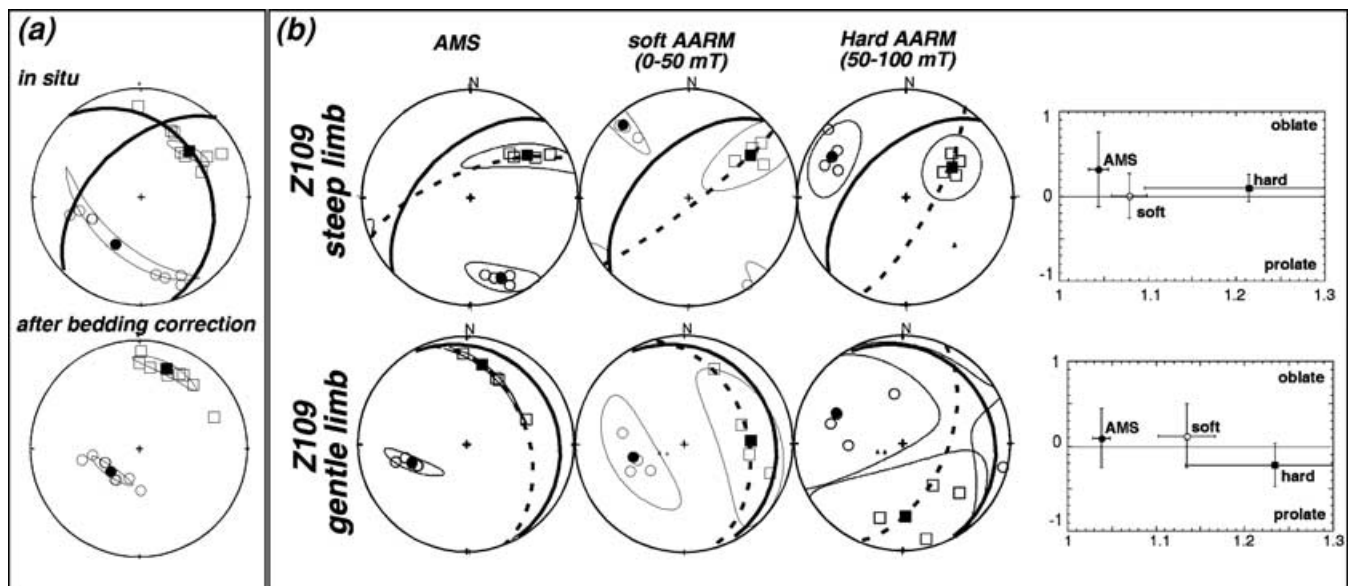


Figure 7. Magnetic fabrics at magnetite-bearing fold Z109. Same legend as in Fig. 6. Tensorial mean (black symbols) are plotted in order to visualize the scattering. (a) AMS in both limbs in geographic coordinates and after untilting the bedding. We thus see that AMS foliation is pre-tilting. (b) AMS and partial AARMs limb by limb.

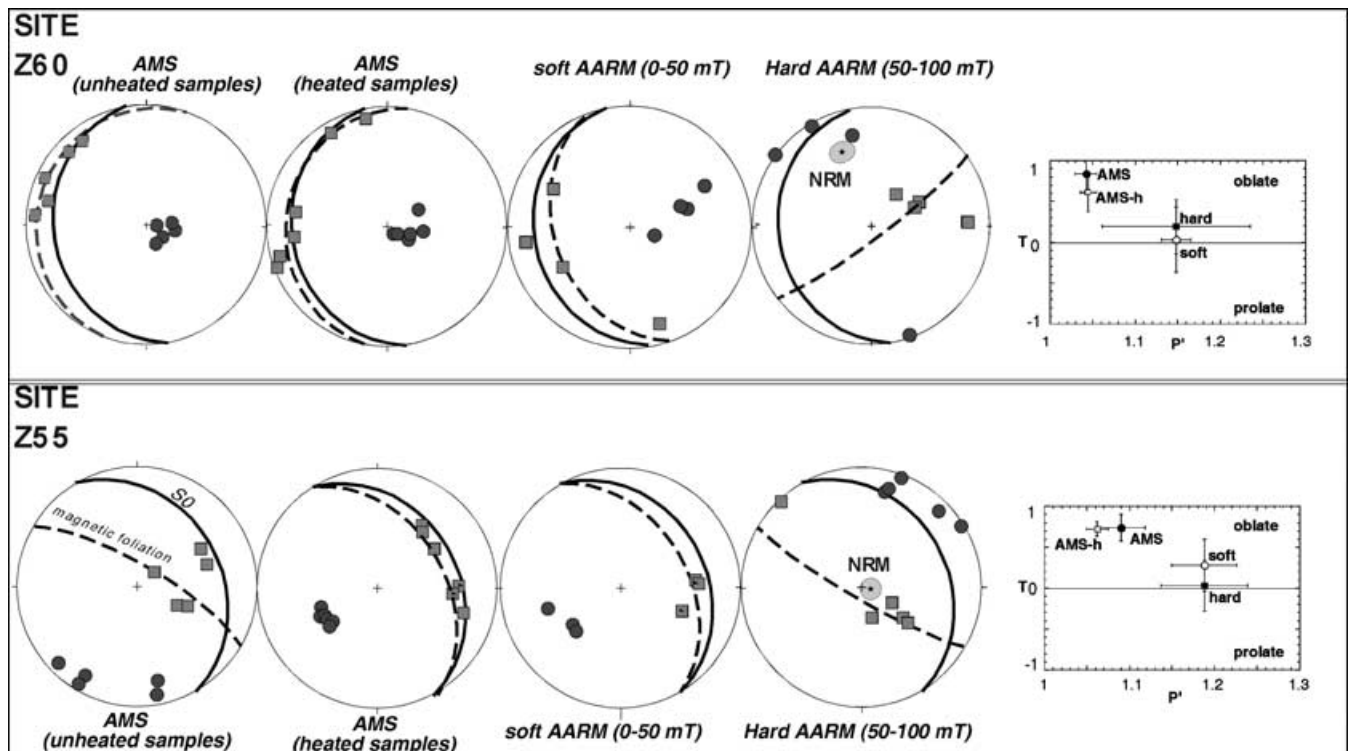


Figure 8. Magnetic fabrics (AMS, soft AARM; hard AARM) at greigite-bearing sites Z60 (a) and Z55 (b). Same legend as in Fig. 6. Note that AMS of heated samples (heating at 700°C under air and cooling in magnetic shielded oven), as well as AMS, soft AARM and hard AARM of unheated samples, are presented. The intermediate temperature component of NRM is shown for hard AARM.

For greigite-bearing sites Z55 and Z60 (Fig. 8), we also measured AMS after heating samples at 700°C. At site Z60, AMS foliations of unheated and heated samples are more or less parallel to bedding. Note however that AMS lineations of heated and unheated samples change significantly. Soft AARM is too scattered to define a foliation, but the rough trend is apparently different both to bedding and AMS foliation. Hard AARM foliation is almost perpendicular to bedding. Anisotropy parameters are weakly anisotropic and oblate for AMS of heated and unheated samples, while they are triaxial and more anisotropic for soft and hard AARM. At site Z55, AMS foliation is rather scattered but largely oblique to bedding. Interestingly, AMS of heated samples groups better and shows very different behavior: its foliation is parallel to bedding. Soft AARM resembles AMS of heated samples. Conversely, hard AARM foliation is close to AMS of unheated samples, and perpendicular to bedding. At site Z55, we know that magnetite and greigite carry magnetic susceptibility. Since greigite is destroyed by *ca.* 400°C, we suggest that AMS of unheated samples and hard AARM are likely carried by greigite, while soft AARM and AMS of heated samples are carried by magnetite. Anisotropy parameters display the same trend than those of site Z60.

DISCUSSION

In these weakly strained sandstones from Makran, we documented composite magnetic fabrics that are distinguishably different each other. It is first questionable how reliable these fabrics are. First, we explore whether magnetic fabrics are independent from each other. It is well known that when magnetic foliations are slightly oblique to each other, then the magnetic lineation trends parallel to the intersection of these magnetic foliations (e.g. Housen *et al.* 1993). In

our data set, this effect is only suggested within the steep limb of fold Z109 (Fig. 7) where the magnetic lineation is parallel to the intersection of AMS and soft and hard AARM foliations. Another possible effect of interacting magnetic fabrics is an apparent relationship between magnetic foliation. Such an effect is suggested at site Z55 because AMS foliation of unheated samples is apparently between the foliations of hard and soft AARM (Fig. 8B). Despite these two relationships, the absence of clear interaction between magnetic fabrics suggests that AMS and soft and hard AARM measure distinct magnetic grain populations. It is tempting to say that the AMS grain fraction is predominantly coarse while the hard AARM reflects mainly fine grains. Distinct peaks in partial ARM coercivity spectra support the existence of several grain fractions.

Second, we investigate a possible relationship between the natural remanent magnetization (NRM) and magnetic fabric. Such interaction is possible, although rarely documented (e.g. Rochette *et al.* 1992). However, NRM-induced deviation should be considered when interpreting hard AARM as this property is dominated by a fine grain fraction, as is NRM. Hard AARMs are characterized by normal-to-bedding foliations and steeply dipping magnetic lineations. A preliminary palaeomagnetic investigation on sites Z55, Z60, Z64 and Z71 defined an intermediate temperature (~200°C–500°C) component of NRM (Figs 6 and 8). This component of NRM is roughly close to hard AARM K_1 or K_3 within 20–30 degrees. It is also noticeable that the plane K_1 – K_3 contains the NRM component. On the basis of this relationship, an interaction between NRM and hard AARM is possible. However, it is difficult to explain why hard AARM foliation is perpendicular to bedding, as there is no relationship between bedding and NRM. Note that there is no apparent relationship between NRM and other magnetic fabrics (AMS and soft AARM).

The composite magnetic fabrics from this study can originate from sedimentary or tectonic processes. In rocks from Makran, a preliminary investigation on about 500 samples indicates that AMS is of tectonic origin (Aubourg *et al.* 2001). A tectonic imprint is also inferred by Bakhtari *et al.* (1998) who reported a systematic tectonic-related AMS in equivalent rocks from Zagros. At fold Z109, we have an additional indication that AMS is not sedimentary in origin. At this fold, AMS foliations in the two limbs are oblique to bedding and poles of AMS foliation group well after restoring bedding to horizontal (Fig. 7a). Pre-tilting and homogeneous oblique AMS foliations taken in several strata cannot be explained by a sedimentary process such as cross bedding. If AMS is pre-tilting at this fold, it seems that hard AARM is post-tilting, ruling out a sedimentary origin. An additional clue for tectonic origin of composite magnetic fabric comes from a comparison of the strike of hard AARM foliations and fold axes. The strikes of hard AARM foliations from sites Z55, Z60 and Z109 are parallel to fold axes, while those from sites Z64 and Z71 are more or less perpendicular. Therefore, we propose that tectonic processes control AMS, hard AARM, and probably soft AARM.

CONCLUSIONS

We give evidence for composite magnetic fabrics in weakly strained sandstones by comparing AMS and partial AARM. We list here a summary of results found in this study:

- (i) Ubiquitous magnetite and locally, greigite control the low field magnetic susceptibility and anhysteretic remanent magnetization of Makran sandstones;
- (ii) Coercivity spectra of partial ARM suggest that grain size distribution of magnetite and greigite is not broad and not unimodal;
- (iii) Soft (0–50 mT) and hard (50–100 mT) partial AARM are reliable techniques where no bias has been detected;
- (iv) Quantitatively, we see the following relationship of corrected degree of anisotropy $P'_{\text{AMS}} \approx 1.04 < P'_{\text{softAARM}} \approx 1.11 < P'_{\text{hardAARM}} \approx 1.19$. AMS is oblate ($T \approx 1$ while partial AARM are generally triaxial ($T \approx 0$)).
- (v) We suggest that AMS, soft AARM and hard AARM measure distinct magnetic fabrics without apparent interactions.
- (vi) A possible relationship between natural remanent magnetization (NRM) and hard AARM is suggested.
- (vii) AMS foliation can be oblique to bedding without any indication of sedimentary features. Such obliquity is pre-tilting at fold Z109.
- (viii) Soft AARM foliation is generally slightly oblique to AMS foliation and bedding.
- (ix) Hard AARM foliation is strongly oblique to AMS and soft AARM foliation, and it is roughly perpendicular to bedding. Its geometry in a fold suggests a post-tilting acquisition.

Previous studies in thrust belt showed that magnetic foliations are often parallel to bedding and more rarely perpendicular to bedding. Our study reveals the composite nature of the magnetic foliation in weakly strained sandstones: coarse and fine grains make respectively a foliation parallel and perpendicular to bedding. We propose that these steep magnetic foliations reflect probably a tectonic event.

ACKNOWLEDGMENTS

We thank C. Bodard who carried out and tested the partial AARM measurements. P. Rochette and an anonymous reviewer provided great help to improve this manuscript.

REFERENCES

- Aubourg, C., Rochette, P. & Bergmüller, F., 1995. Composite magnetic fabric in weakly deformed black shales, *Phys. Earth planet. Inter.*, **87**, 267–278.
- Aubourg, C., Hebert, R., Jolivet, L. & Cartayrade, G., 2000. The magnetic fabric of metasediments in a detachment zone: the example of Tinos Island, *Tectonophysics*, **321**, 219–236.
- Aubourg, C., Smith, B., Bakhtari, H., Guya, N. & Lallemand, S., 2001. Magnetic fabric of recent weakly strained clastics through Zagros-Makran syntaxis (SE Iran), *Geophysical Research Abstract*, 3 (EGS 26th General Assembly).
- Bakhtari, H., Frizon de Lamotte, D., Aubourg, C. & Hassanzadeh, J., 1998. Magnetic fabric of Tertiary sandstones from the Arc of Fars (Eastern Zagros, Iran), *Tectonophysics*, **284**, 299–316.
- Borradaile, G.J. & Henry, B., 1997. Tectonic applications of magnetic susceptibility and its anisotropy, *Earth Sci. Rev.*, **42**, 49–93.
- Daly, L. & Zinsser, H., 1973. Étude comparative des anisotropies de susceptibilité et d'aimantation rémanente isotherme. Conséquences pour l'analyse structurale et le paléomagnétisme, *Ann. Géophys.*, **29**, 189–200.
- Day, R., Fuller, M. & Schmidt, V.A., 1977. Hysteresis properties of titanomagnetite: grain size and compositional dependence, *Phys. Earth planet. Inter.*, **13**, 260–267.
- Graham, J.W., 1954. Magnetic susceptibility anisotropy, an unexploited petrofabric element, *Bull. geol. Soc. Am.*, **65**, 1257–1258.
- Housen, B.A., Richter, C. & Van der Pluijm, B.A., 1993. Composite magnetic anisotropy fabrics: experiments, numerical models, and implications for the quantification of rocks fabrics, *Tectonophysics*, **200**, 1–12.
- Hrouda, F., 1982. Magnetic anisotropy of rocks and its application in geology and geophysics, *Geophys. Surv.*, **5**, 37–82.
- Jackson, M., 1991. Anisotropy of Magnetic Remanence: a brief review of mineralogical sources, physical origins, and geological applications, and comparison with susceptibility anisotropy, *Pageoph*, **136**, 1–26.
- Jackson, M., Gruber, W., Marvin, J. & Banerjee, S.K., 1988. Partial anhysteretic and its anisotropy: applications and grain-size-dependence, *Geophys. Res. Lett.*, **15**, 440–443.
- Jelinek, V., 1977. The statistical theory of measuring anisotropy of magnetic susceptibility on groups of specimens and its application, *Geofyzyka*, 1–88.
- Jelinek, V., 1978. Statistical processing of anisotropy of magnetic susceptibility measured on group of specimen, *Studia Geoph. et Geod.*, **22**, 50–62.
- Jelinek, V., 1993. Theory and measurement of the anisotropy of isothermal remanent magnetization of rocks, *Travaux Géophysique*, **XXXVII** (1993–96), 124–134.
- Lowrie, W., 1990. Identification of ferromagnetic minerals in rock by coercivity and unblocking temperature properties, *Geophys. Res. Lett.*, **17**, 159–162.
- McCabe, C., Jackson, M. & Ellwood, B.B., 1985. Magnetic anisotropy in the Trenton limestone: results of a new technique, anisotropy of anhysteretic susceptibility, *Geophys. Res. Lett.*, **12**, 333–336.
- McCall, G.J., 1997. The geotectonic history of the Makran and adjacent areas of Southern Iran, *J. Asian earth sci.*, **15**, 517–531.
- Robion, P., Averbuch, O. & Sintubin, M., 1999. Fabric development and metamorphic evolution of Lower Paleozoic slaty rocks from the Rocroi massif (French-Belgian Ardennes): new constraints from magnetic fabrics, phyllosilicate preferred orientation and illite crystallinity data, *Tectonophysics*, **309**, 257–273.
- Rochette, P., Jackson, J. & Aubourg, C., 1992. Rock magnetism and the interpretation of anisotropy of magnetic susceptibility, *Rev. Geophys.*, **30**, 209–226.
- Rochette, P., Aubourg, C. & Perrin, M., 1999. Is this magnetic fabric normal? A review and case studies in volcanic formation, *Tectonophysics*, **307**, 219–234.
- Sagnotti, L. & Winkler, A., 1999. Rock magnetism and paleomagnetism of greigite bearing mudstones in the Italian peninsula, *Earth planet. Sci. Lett.*, **165**, 67–80.

- Stephenson, A., 1993. Three axis static alternating field demagnetization of rocks and the identification of natural remanent magnetization, gyroremanent magnetization, and anisotropy, *J. geophys. Res.*, **96**, 373–381.
- Stephenson, A., Sadikun, S. & Potter, D.K., 1986. A theoretical and experimental comparison of the anisotropies of magnetic susceptibility and remanence in rocks and minerals, *Geophys. J. R. astr. Soc.*, **84**, 185–200.
- Tarling, D.H. & Hrouda, F., 1993. *The Magnetic Anisotropy of Rocks*, Chapman & Hall, London.
- Tauxe, L., Constable, C., Stokking, L. & Badgley, C., 1990. Use of anisotropy to determine the origin of characteristic remanence in the Siwalik red bed of northern Pakistan, *J. geophys. Res.*, **95**, 4391–4404.
- Trindade, R.I.F., Raposo, M.I.B., Ernesto, M. & Siqueira, R., 1999. Magnetic susceptibility and partial anisotropic remanence anisotropies in the magnetite-bearing granite pluton of Tourao, NE Brazil, *Tectonophysics*, **314**, 443–468.
- Werner, T. & Borradaile, G.J., 1996. Paleoremanence dispersal across a transpressed Archean terrain: deflection by anisotropy or by late compression?, *J. geophys. Res.*, **101**, 5531–5545.